



A leaky mutation in *CD3D* differentially affects $\alpha\beta$ and $\gamma\delta$ T cells and leads to a $T\alpha\beta^-T\gamma\delta^+B^+NK^+$ human SCID

Juana Gil,¹ Elena M. Busto,² Beatriz Garcillán,² Carmen Chean,¹ Maria Cruz García-Rodríguez,³ Andrea Díaz-Alderete,¹ Joaquín Navarro,¹ Jesús Reiné,² Angeles Mencía,⁴ Dolores Gurbindo,¹ Cristina Beléndez,¹ Isabel Gordillo,¹ Marlena Duchniewicz,⁵ Kerstin Höhne,⁵ Félix García-Sánchez,⁶ Eduardo Fernández-Cruz,¹ Eduardo López-Granados,³ Wolfgang W.A. Schamel,⁵ Miguel A. Moreno-Pelayo,⁴ María J. Recio,² and José R. Regueiro²

¹Gregorio Marañón University Hospital, Madrid, Spain. ²School of Medicine, Complutense University, i+12 and RIER, Madrid, Spain.

³La Paz University Hospital, Madrid, Spain. ⁴Ramón y Cajal University Hospital, IRYCIS and CIBERER, Madrid, Spain.

⁵Faculty of Biology, Centre of Chronic Immunodeficiency (CCI), BIOS Centre for Biological Signaling Studies, University of Freiburg and Max Planck Institute of Immunobiology and Epigenetics, Freiburg, Germany. ⁶Blood Transfusion Centre, Madrid, Spain.

T cells recognize antigens via their cell surface TCR and are classified as either $\alpha\beta$ or $\gamma\delta$ depending on the variable chains in their TCR, α and β or γ and δ , respectively. Both $\alpha\beta$ and $\gamma\delta$ TCRs also contain several invariant chains, including CD3 δ , which support surface TCR expression and transduce the TCR signal. Mutations in variable chains would be expected to affect a single T cell lineage, while mutations in the invariant chains would affect all T cells. Consistent with this, all CD3 δ -deficient patients described to date showed a complete block in T cell development. However, CD3 δ -KO mice have an $\alpha\beta$ T cell-specific defect. Here, we report 2 unrelated cases of SCID with a selective block in $\alpha\beta$ but not in $\gamma\delta$ T cell development, associated with a new splicing mutation in the *CD3D* gene. The patients' T cells showed reduced *CD3D* transcripts, CD3 δ proteins, surface TCR, and early TCR signaling. Their lymph nodes showed severe T cell depletion, recent thymus emigrants in peripheral blood were strongly decreased, and the scant $\alpha\beta$ T cells were oligoclonal. T cell-dependent B cell functions were also impaired, despite the presence of normal B cell numbers. Strikingly, despite the specific loss of $\alpha\beta$ T cells, surface TCR expression was more reduced in $\gamma\delta$ than in $\alpha\beta$ T cells. Analysis of individuals with this *CD3D* mutation thus demonstrates the contrasting CD3 δ requirements for $\alpha\beta$ versus $\gamma\delta$ T cell development and TCR expression in humans and highlights the diagnostic and clinical relevance of studying both TCR isotypes when a T cell defect is suspected.

Introduction

T lymphocytes recognize antigens by means of a cell surface complex termed the TCR. The TCR contains 2 variable chains to bind antigens and several invariant chains to support variable chains and to transduce the signals required for T cell differentiation and antigen recognition (1). The invariant chains present in the human TCR are CD3 γ , CD3 δ , CD3 ϵ , and TCR ζ (CD247) (Figure 1A). T lymphocytes belong to either the $\alpha\beta$ or the $\gamma\delta$ lineage according to the types of variable chains incorporated into their TCR, α and β or γ and δ , respectively.

Mutations in *TCR* or *CD3* genes selectively impair T cell development (2). Unless hematopoietic stem cells are replaced, the mutations frequently cause early-onset SCID and death. When a variable chain such as TCR α is affected, only $\alpha\beta$ T cells are impaired, as shown recently (3). When an invariant chain is affected, both $\alpha\beta$ and $\gamma\delta$ T cells are either absent, as observed in CD3 δ or CD3 ϵ deficiency (4, 5), or reduced, as reported for CD3 γ or TCR ζ deficiency (6, 7). These immunophenotypes are described as $T^-B^+NK^+$ or $T^+B^+NK^+$, respectively. However, no selective $\alpha\beta$ or $\gamma\delta$ T cell-deficient patients have been reported

for invariant TCR chain deficiencies. We describe 2 SCID cases with severe selective $\alpha\beta$ T lymphopenia ($T\alpha\beta^-T\gamma\delta^+B^+NK^+$) caused by a leaky mutation in *CD3D* that titrated the differential CD3 δ requirements for human $\alpha\beta$ and $\gamma\delta$ T lymphocyte development and TCR expression in vivo.

Results and Discussion

Case reports. Two unrelated children from nonconsanguineous Ecuadorian parents showed common clinical and immunophenotypic features. They presented at 13 (AIII.1) and 5 (BII.2) months of age with SCID features, $T^+B^+NK^+$ phenotype, low CD3 expression, strongly impaired proliferative responses to T cell mitogens (Table 1), severe lymph node T cell depletion, and lack of activated germinal centers. Both received conditioning and haploidentical CD34⁺ peripheral blood hematopoietic stem cell transplantation at 23 and 8 months, respectively.

Patient AIII.1 was admitted with failure to thrive, bronchopneumonia, severe diarrhea caused by strains of *Salmonella*, *Campylobacter*, and *Cryptosporidium*, oral candidiasis, and atopic dermatitis. CMV and EBV were negative by PCR. Neutrophil, lymphocyte, and platelet numbers and serum and urine biochemistry were normal, including Ig levels except IgE, which was strongly increased (Table 1). NK cell function was normal, whereas T cell-dependent B cell function was impaired. Specific Abs against protein antigens were not induced upon vaccination

Authorship note: Juana Gil and Elena M. Busto are co-first authors. María J. Recio and José R. Regueiro are co-senior authors.

Conflict of interest: The authors have declared that no conflict of interest exists.

Citation for this article: *J Clin Invest.* 2011;121(10):3872–3876. doi:10.1172/JCI44254.

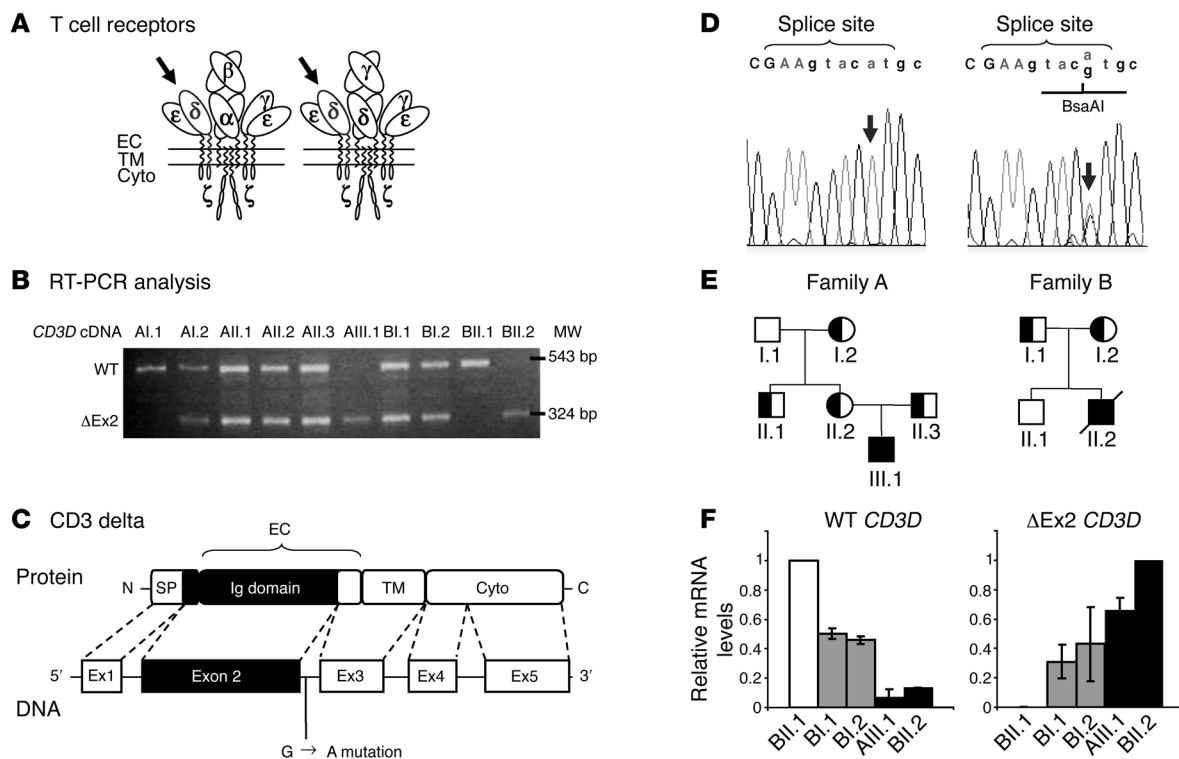


Figure 1

CD3D mutation analysis. (A) Structure of the 2 TCR that incorporate the CD3 δ chain (arrows). EC, extracellular region; TM, transmembrane region; Cyto, cytoplasmic region. (B) *CD3D* RNA RT-PCR amplification products. Δ Ex2 bands lack exon 2 (C) *CD3 δ* protein and gene structure with localization of the G \rightarrow A mutation. SP, signal peptide. (D) *CD3D* electropherograms showing the IVS2+5G \rightarrow A mutation (arrow) in patient AIII.1 (left) and his father (right), and the BsaAI restriction site. Exon/intron sequences are in upper/lower case, respectively. (E) Genetic pedigrees. Circles indicate females; squares indicate males (slashes indicate deceased). Solid symbols denote homozygosity; half-solid symbols denote heterozygosity. (F) WT and Δ Ex2 *CD3D* transcript levels relative to *CD3E* by quantitative RT-PCR in PBMCs using exon-specific primers and isoform-specific probes. Data represent mean \pm SD of at least 2 experiments, relative to the highest value in each data set, which is shown as 1.

and were not detected against common pathogens or autoantigens, whereas natural (IgM) Abs against polysaccharides such as isoagglutinins and heterophile Abs were normal. The patient required total parenteral nutrition, specific antimicrobials, and i.v. Ig therapy. Absence epilepsy developed at 16 months. Sclerosing cholangitis was observed before receiving a maternal transplant. At 4 years of age, he is doing well, with mixed chimerism.

Patient BII.2 was admitted with fever, prostrating diarrhea, and respiratory distress. Urine CMV and nasal adenovirus, discrete lymphopenia, and severe hypogammaglobulinemia were observed. A protein-losing enteropathy was diagnosed, and he started on i.v. Ig and prophylactic Septrin, but developed several lymphadenopathies. After an initial improvement, respiratory function deteriorated and bronchoalveolar CMV was identified, which required antivirals. He underwent paternal transplantation with full chimerism in 3 weeks, but returned to the intensive care unit with respiratory distress, hemodynamic instability, encephalopathy, and liver failure with secondary coagulopathy, and died following multiorgan failure. Necropsy evidenced a rudimentary thymus with conserved reticular structure but complete depletion of lymphocytes and Hassall corpuscles. CMV identified in the liver, brain, heart, and lung was the likely cause of disease.

A novel mutation in CD3D. The decreased CD3 expression observed in both patients suggested a potential TCR defect. We thus analyzed *CD3* and *CD247* RNA by RT-PCR and found short *CD3D*

PCR products in several family members (Figure 1B). Sequencing revealed a complete in-frame deletion of exon 2, which encodes the extracellular Ig-like domain of CD3 δ (Figure 1C).

Exon skipping suggested a potential splicing defect. Genomic DNA sequencing detected a homozygous G-to-A mutation at position +5 in the 5' splice donor site of intron 2 (IVS2+5G \rightarrow A; Figure 1D). The mutation abrogated a restriction site for the enzyme BsaAI, which was used to follow its segregation (Figure 1E). The mutation was causing the immunodeficiency, as it was not found in 140 Spanish or Ecuadorian healthy donors, and its location is strictly conserved in mammals (Supplemental Figure 1; supplemental material available online with this article; doi:10.1172/JCI44254DS1).

The patients' parents were carriers of the same *CD3D* mutation and had a similar geographic origin, indicating that they likely shared a founder mutant allele. The analysis of polymorphic microsatellite markers spanning the *CD3* region (which contains *CD3G*, *CD3D*, and *CD3E*) confirmed the presence of a shared core haplotype associated with the mutation (Supplemental Figure 2).

From the data in Figure 1B, it seemed that some normal PCR products might be present in the patients, indicating that the mutation did not abrogate normal splicing at the *CD3D* locus, as shown in similar intronic mutations (8). To analyze *CD3D* splicing, quantitative RT-PCR relative to *CD3E* was performed. The results confirmed the presence of small amounts of WT *CD3D* transcripts in the patients (Figure 1F).



Table 1
Lymphocyte studies in 2 affected children with the SCID disorder

Variables	Patient AIII.1	Patient BII.2	Normal range
Lymphocyte number/μl at	13 months	6 months	9–15 months
T (CD3 ⁺)	400	787	1600–6700
B (CD19 ⁺)	1987	2183	600–2700
NK (CD3-CD16 ⁺ /CD56 ⁺)	636	537	180–1200
T cell proliferation (cpm)^A			
Medium	201	851	<1000
Phytohemagglutinin	2242	2562	>80,000
Anti-CD3	8020	1327	>50,000
Serum Ig (mg/dl)			
IgG	1170	40 ^B	310–1380
IgA	156	38	30–120
IgM	121	44	50–120
IgE (IU/ml)	4019	3	0–120
IgG1	957	ND ^{B,C}	430–900
IgG2	458	ND ^{B,C}	30–390
IgG3	<6.4	ND ^{B,C}	10–80
IgG4	50	ND ^{B,C}	10–65
Functional Abs		ND ^{B,C}	
Natural Abs (titer)			
Heterophile Abs	1/256		\geq 1/64
Isohemagglutinins (anti-B)	1/16		\geq 1/8
Infectious specificities ^D	Neg		–
Vaccination responses	Before/After		After
Hepatitis B (IU/ml)	NAV ^C / 0		>10
Tetanus toxoid (IU/ml)	0.01 / 0.03		0.04–3.92
Influenza (HI) ^E	8/16		>32
NK cell cytotoxicity (% lysis)^F		ND ^C	
100:1	34		30–86
50:1	21		20–84
12:1	8		1–57

^AH³-thymidine uptake in response to mitogens. ^BProtein-losing enteropathy. ^CNot done or not available (neonatal vaccination). ^DIgG anti-CMV, EBV, HSV, VZV, HIV, HAV, rubella, measles, toxoplasma, and IgE anti-aspergillus. ^EHemagglutination inhibition. ^FAt the indicated effector/target ratios.

From these results, we concluded that a homozygous IVS2+5G→A mutation strongly impaired (around 10-fold), but did not abrogate, normal *CD3D* splicing in both patients.

Reduced *CD3D* protein. The small levels of WT *CD3D* transcripts were found to be sufficient to encode for half-normal levels of WT *CD3D* proteins in the patients' T cells as shown in family B by Western blotting (Figure 2) or intracellular flow cytometry (Supplemental Figure 3A). In contrast, the dominant Δ Ex2 *CD3D* transcripts did not give rise to detectable levels of the predicted headless *CD3D* chain, despite being readily detected after transfection in non-T cells (Figure 2B).

We cannot exclude that small amounts of Δ Ex2 *CD3D* might be expressed below the detection limit of Western blotting. However, when overexpressed in *Drosophila* cells, Δ Ex2 did not compete with WT *CD3D* in the formation of a TCR complex (Supplemental Methods and Supplemental Figure 4).

From these studies, we concluded that the immunodeficiency was associated with reduced levels of normal *CD3D*.

Immunological characteristics. The human *CD3D* chain is incorporated into both TCR $\alpha\beta$ and TCR $\gamma\delta$ (Figure 1A). To establish how the *CD3D* mutation affected lymphocyte differentiation, the

numbers of $\alpha\beta$ T cells and $\gamma\delta$ T cells were determined in both patients (Figure 3A). The results showed a severe selective reduction in peripheral blood $\alpha\beta$ T lymphocyte numbers (both CD4⁺ and CD8⁺; Supplemental Figure 5), close to 10-fold compared with the median value of healthy age-matched controls. In contrast, $\gamma\delta$ T cells as well as B and NK lymphocytes were detected in normal numbers (T $\alpha\beta$ ⁻T $\gamma\delta$ ⁺B⁺NK⁺ phenotype; Figure 3A and Table 1). A possible role for CMV in $\gamma\delta$ T cell predominance was proposed in some SCID reports (9) but not in others (10). However, CMV-induced $\gamma\delta$ T expansion was excluded in patient AIII.1.

The reduction caused by the *CD3D* mutation in $\alpha\beta$, but not $\gamma\delta$, T lymphocyte numbers suggested a differential *CD3D* requirement for TCR expression or function in $\alpha\beta$ versus $\gamma\delta$ T cells. Counterintuitively, TCR expression was around 2-fold lower in $\gamma\delta$ than in $\alpha\beta$ T cells from the patients using different TCR- or *CD3*-specific mAbs, both in primary (Figure 3B) and in cultured T cells (Supplemental Figure 3B). TCR downregulation after engagement by anti-CD3, however, was similar in both T cell lineages (Supplemental Figure 6A). In contrast, early activation events such as CD69 or CD25 induction were strongly reduced (Figure 3C and Supplemental Figure 6, B and C). $\alpha\beta$ and $\gamma\delta$ T cells were nevertheless capable of normal anti-CD3- or phytohemagglutinin-induced short-term proliferation on a per-cell basis (5 days; Supplemental Figure 6D). This was confirmed in culture using allogeneic feeder cells (Figure 3D). However, after day 25 in the same cultures, $\alpha\beta$, but not $\gamma\delta$, T cells showed impaired growth relative to a control. Therefore, the *CD3D* mutation impaired TCR expression and several functions in $\gamma\delta$ and $\alpha\beta$ T cells, albeit with some contrasting effects: lower TCR expression by $\gamma\delta$ T cells but lower in vitro long-term survival of $\alpha\beta$ T cells. *CD3D* has been reported to bind less strongly to the TCR $\gamma\delta$ than to the TCR $\alpha\beta$ heterodimer (11), offering a potential mechanism for the observed differential surface levels of TCR in $\gamma\delta$ versus $\alpha\beta$ T cells when *CD3D* is reduced.

The thymus was normal in size at diagnosis (Supplemental Figure 7). To study its function, several studies were performed, including analyses of recent thymic emigrants defined as CD4⁺CD45RA⁺CD31⁺ cells, CD45RA⁺ (naive) and CD45RO⁺ (memory) T cells, CD25 expression; *TCRB* clonality, and TCRV β usage (Supplemental Figures 8 and 9). The results indicated that the patients' thymuses produced very few $\alpha\beta$ T lymphocytes, and most of these had differentiated into effector memory T cells with an activated phenotype and an oligoclonal TCRV β repertoire. They may have contributed to the observed in vivo Th2 features in patient AIII.1 (hyper-IgE, eosinophilia, and atopic dermatitis). Similar Th2 immunopathology has been observed in lymphopenic patients with Omenn-like syndrome associated with several primary immunodeficiencies (12) and in mice with partial T cell immunodeficiency (13).

These results indicated that the *CD3D* splicing mutation strongly impaired $\alpha\beta$, but not $\gamma\delta$, T lymphocyte selection in the thymus, resembling the phenotype of *CD3D*-KO mice (14). In contrast,

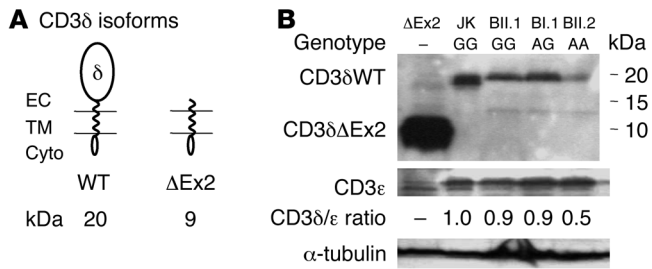


Figure 2
CD3δ protein analysis. (A) WT CD3δ and the predicted truncated isoform (ΔEx2). (B) Western blotting analysis of CD3δ isoforms in lysates from ΔEx2-transfected 293T cells, Jurkat cells (JK), or T cell lines with the indicated *CD3D* IVS2+5 genotypes using APA1/2 (anti-human CD3δ cytoplasmic tail), anti-CD3ε, or anti-tubulin. The numbers under each lane indicate CD3δWT band intensity relative to CD3ε.

human complete CD3δ immunodeficiencies uniformly lack all T cells (4, 5). Therefore, the leaky mutation, which we believe to be novel, reveals that human αβ and γδ T lymphocytes have differential CD3δ requirements for selection that have not been described for other invariant chains (CD3γ, CD3ε, or TCRζ; Supplemental Table 1). The Tαβ⁺Tγδ⁺B⁺NK⁺ phenotype has been reported recently in 2 children with TCRα deficiency (3). However, those patients remained relatively healthy for 6–7 years on antibiotic prophylaxis before transplantation; they had activated germinal centers and specific Ab responses against vaccines and autoantigens, likely due to γδ T cell help by homology with the mouse model. The leaky CD3δ

SCID patients reported here required very early transplantation (before 1–2 years), lacked germinal centers, and showed very poor T cell-dependent B cell function, perhaps due to the signaling impairment observed also in their γδ T cells (Figure 3C). Thus, CD3δ levels are sufficient for selection, but not for normal function of γδ T cells, as described for CD4⁺ T cells in Zap70 SCID patients (2).

Two mechanisms may be proposed to explain the selective effect of low CD3δ levels in αβ T lymphocyte development. One is impaired assembly or signaling of the immature precursor of the TCRαβ termed the pre-TCR (15). The second one is impaired signaling through the mature TCRαβ due to reduced interactions of CD3δ with an evolutionarily conserved motif in the TCRα chain membrane-proximal constant region termed the α-chain connecting peptide (16).

Together, the results showed that the leaky *CD3D* mutation reduced CD3δ chains, which in turn blocked αβ rather than γδ T cell selection. In mature T cells, TCRγδ expression was more impaired than TCRαβ expression, but early signaling through both was similarly impaired.

Methods

Further information can be found in Supplemental Methods.

Mutation detection. *CD3* amplimers were generated by RT-PCR of PBMC RNA with specific primers (Supplemental Tables 2 and 3). *CD3D* exons and flanking intronic sequences were amplified from leukocyte DNA by PCR using specific primers and sequenced following standard techniques. Screening for the IVS2+5G→A mutation was performed by RFLP using *Bsa*AI (New England Biolabs). Ecuadorian DNA samples were provided by Antonio Arnaiz-Villena (Complutense University).

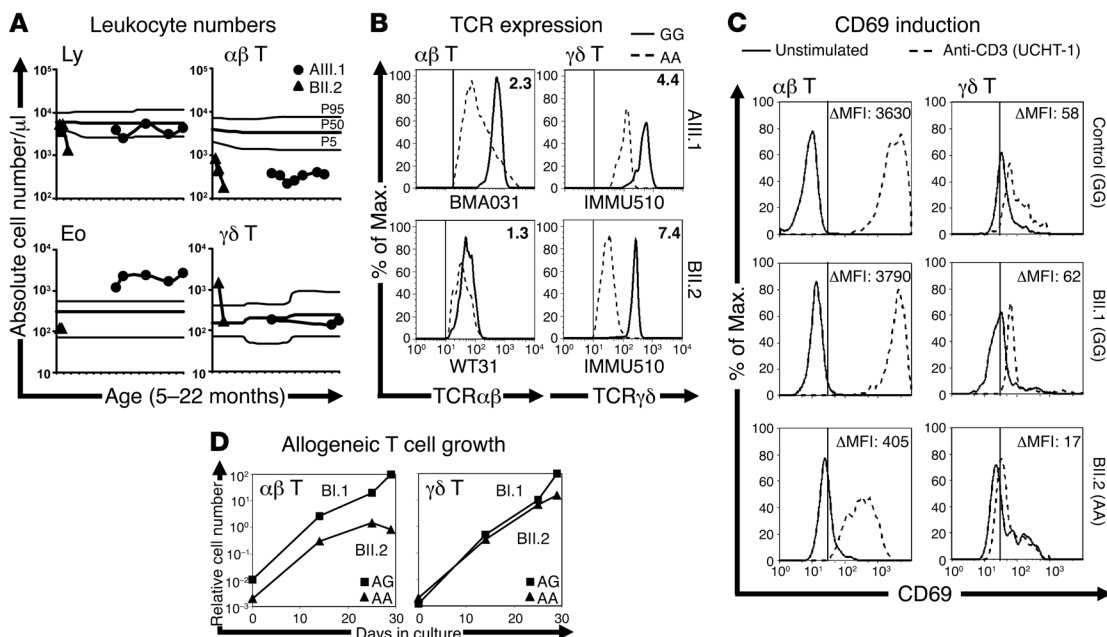


Figure 3
T lymphocyte analysis. (A) Absolute cell numbers in patients plotted as a function of age in comparison with the normal age-matched distribution (P5, P50, and P95). The leukocyte subsets are lymphocytes (Ly), eosinophils (Eo), αβ T (CD4⁺+CD8^{bright}), and γδ T (11F2⁺) cells. (B) TCRαβ and TCRγδ cell surface expression in primary lymphocytes from the patients (dashed lines, AA genotype) in comparison with controls (solid lines, GG genotype), measured using the indicated TCRαβ- and TCRγδ-specific mAb. The numbers in each histogram indicate MFI ratios between control and patient. (C) CD69 induction (geometric MFI increments) after 24 hours in anti-CD3-stimulated (dashed lines) versus unstimulated (solid lines) primary αβ T (CD4⁺) or γδ T (IMMU510⁺) lymphocytes with the indicated genotypes. (D) Patient T cell growth in feeder cell cultures expressed as a percentage of carrier BI.1 T cell numbers.



Quantitative PCR. TaqMan PCR of PBMC cDNA was done using CD3D WT- or ΔEx2-specific primers and probes (Supplemental Table 4). Samples were normalized to the Ct of CD3E-specific primers and probe 49 from the Universal ProbeLibrary Human (Roche) and to the highest value in each data set, which is shown as 1.

Transfections and Western blotting. 293T cells were transiently transfected using lipofectamine (Invitrogen) with 2 μg of plasmid pIRES-GFP1a (Invitrogen) containing ΔEx2 CD3D cDNA, lysed and analyzed by Western blotting, together with cultured T cells, using APA1/2 (mouse anti-CD3δ cytoplasmic tail IgG mAb; provided by Balbino Alarcón, Centro de Biología Molecular, Madrid, Spain) or M20epsilon (goat anti-CD3ε IgG; Santa Cruz Biotechnology Inc.).

Immunological investigations. Lymphocyte phenotype was determined by flow cytometry using anti-CD3 (Leu4/SK7), anti-CD69 (L78), anti-CD19 (SJ25C1), anti-CD16 (73.1), anti-CD56 (NCAM16.2), and anti-TCRγδ (11F2) from BD Biosciences; and anti-TCRαβ (BMA031 or WT31), anti-TCRγδ (IMMU510), anti-CD4 (13B8.4), and anti-CD8 (B9.11) from Beckman Coulter Immunotech. T cell function was tested by standard overnight H³-thymidine uptake assays (1 μCi/well) by culturing 10⁵ PBMCs with phytohemagglutinin (1 μg/ml; Sigma-Aldrich) or plastic-bound anti-CD3 (10 μg/ml UCHT-1 from BD) for 72 hours. NK cell function was tested by standard ⁵¹Cr release assays using PBMCs as effectors and K562 cells as targets. Specific lysis was calculated from cpm as 100 × (sample)/(maximum), after correcting for blank measurements.

T cell lines were generated from PBMCs and expanded weekly with irradiated allogeneic feeder cells (PBMCs and EBV-transformed B cells) at 1:5:5 ratios and final 10⁶ cells/ml in IMDM medium (PAA) with 0.1 μg/ml phytohemagglutinin (only at day 0; Sigma-Aldrich), 40 IU/ml rIL-2 (provided by Craig W. Reynolds, Frederick Cancer Research and Development

Center, NCI, NIH, Frederick, Maryland, USA), 10% AB⁺ human serum, and 1% glutamine (Gibco; Invitrogen).

Study approval. The study was conducted according to the principles expressed in the Declaration of Helsinki and approved by the Hospital Clínico Research Ethics Committee, Madrid, Spain. All participants or their guardians provided informed consent for the collection of samples and subsequent analyses.

Statistics. Bar graph data represent mean ± SD. For proliferation and cytotoxicity, median values of triplicates were used.

Acknowledgments

This work was supported by grants from the Spanish NIH (ISCIII – PI080921, PI060057, PI080045, RIER), Ministry of Health (2010 Cohesion Fund for Rare Diseases), Ministry of Science (SAF2011-24235), Fundación Mutua Madrileña, and the Deutsche-Forschungsgemeinschaft (EXC294/BIOSS, SFB620B6). We thank Bruno Hernández, Verónica Pérez-Flores, Alberto C. Guardo, Edgar Fernandez-Malavé, Pilar Perez Breña (National Microbiology Center), and Pieter C.M. Res (University of Amsterdam) for technical support and comments.

Received for publication January 18, 2011, and accepted in revised form August 3, 2011.

Address correspondence to: José R. Regueiro, Inmunología, Facultad de Medicina, Universidad Complutense, 28040 Madrid, Spain. Phone: 34913941642; Fax: 34913941641; E-mail: regueiro@med.ucm.es.

1. Weiss A, Littman DR. Signal transduction by lymphocyte antigen receptors. *Cell*. 1994;76(2):263–274.
2. Notarangelo LD, et al. Primary immunodeficiencies: 2009 update The International Union of Immunological Societies (IUIS) Primary Immunodeficiencies (PID) Expert Committee. *J Allergy Clin Immunol*. 2009;124(6):1161–1178.
3. Morgan NV, et al. Mutation in the TCRα subunit constant gene (TRAC) leads to a human immunodeficiency disorder characterized by a lack of TCRαβ+ T cells. *J Clin Invest*. 2011;121(2):695–702.
4. Dadi HK, Simon AJ, Roifman CM. Effect of CD3delta deficiency on maturation of alpha/beta and gamma/delta T-cell lineages in severe combined immunodeficiency. *N Engl J Med*. 2003;349(19):1821–1828.
5. de Saint Basile G, et al. Severe combined immunodeficiency caused by deficiency in either the delta or the epsilon subunit of CD3. *J Clin Invest*. 2004;114(10):1512–1517.
6. Siegers GM, et al. Different composition of the human and the mouse gammadelta T cell receptor explains different phenotypes of CD3gamma and CD3delta immunodeficiencies. *J Exp Med*. 2007;204(11):2537–2544.
7. Roberts JL, et al. T-B⁺NK⁺ severe combined immunodeficiency caused by complete deficiency of the CD3zeta subunit of the T-cell antigen receptor complex. *Blood*. 2007;109(8):3198–3206.
8. Wada T, et al. Detection of T lymphocytes with a second-site mutation in skin lesions of atypical X-linked severe combined immunodeficiency mimicking Omenn syndrome. *Blood*. 2008;112(5):1872–1875.
9. Ehl S, et al. A variant of SCID with specific immune responses and predominance of γδ T cells. *J Clin Invest*. 2005;115(11):3140–3148.
10. Enders A, et al. A severe form of human combined immunodeficiency due to mutations in DNALigase IV. *J Immunol*. 2006;176(8):5060–5068.
11. Alibaud L, Arnaud J, Llobera R, Rubin B. On the role of CD3d chains in TCRgd/CD3 complexes during assembly and membrane expression. *Scand J Immunol*. 2001;54(1-2):155–162.
12. Ozcan E, Notarangelo LD, Geha RS. Primary immune deficiencies with aberrant IgE production. *J Allergy Clin Immunol*. 2008;122(6):1054–1062.
13. Liston A, Enders A, Siggs OM. Unravelling the association of partial T-cell immunodeficiency and immune dysregulation. *Nat Rev Immunol*. 2008;8(7):545–558.
14. Dave VP, et al. CD3δ deficiency arrests development of the αβ but not the γδ T cell lineage. *EMBO J*. 1997;16(6):1360–1370.
15. Yamasaki S, Saito T. Molecular basis for pre-TCR-mediated autonomous signaling. *Trends Immunol*. 2007;28(1):39–43.
16. Bäckström BT, Müller U, Hausmann B, Palmer E. Positive selection through a motif in the alphabeta T cell receptor. *Science*. 1998;281(5378):835–838.

SUPPLEMENTAL TABLES

Supplemental Table 1. Human TCR complex deficiencies^A

Protein	Gene	Chr.	OMIM	References		Number of patients	
				Complete	Leaky	Complete	Leaky
CD3 γ	<i>CD3G</i>	11	186740	1		5	
CD3 δ	<i>CD3D</i>	11	186790	2,3,4	^B	7	2 ^B
CD3 ϵ	<i>CD3E</i>	11	186830	3	5	3	1
TCR ζ	<i>CD247</i>	1	186780	6	7	1	1
TCR α	<i>TRAC^C</i>	14	186880	8		2	
				Total		18	4

^A Classified as complete or leaky according to the effect of the mutations. Leaky, but not complete, mutations allow for the synthesis of low amounts of the wild type protein.

^B Present manuscript. The GenBank accession no. for the cDNA and genomic DNA mutant sequences are JN392069 and JN392070, respectively.

^C TCR α constant gene segment.

Supplemental Table 2. Primers used for RT-PCR^A

Gene	Primer	Sequence (5' to 3')
<i>CD3G</i>	CD3GF	AAAAAGAATTCTCAATTCCTCCTCAACTC
	CD3GR	AAAAAGGATCCATGGAACAGGGGAAGGG
<i>CD3D</i>	CD3DF	CTGTAGGAATTCACGATGGAACATAGCACGTTTCTC
	CD3DR	CTAGCTCTCGAGTCACTTGTTCCGAGCCCAGTT
<i>CD3E</i>	CD3EF	TTCCTGTGTGGGGTTCAGAAACC
	CD3ER	CCATCAGGCTGAGGAACGATTCT
<i>CD247</i>	CD247F	CTGAGGGAAAGGACAAGATGAAG
	CD247R	AAAGAGTGCAGGGACAACAGTCT

^A OLIGO Primer Analysis Software version 7 from Molecular Biology Insights was run for the following gene sequences (GenBank accession no.): *CD3G* (NM_000073), *CD3D* (NM_000732), *CD3E* (NM_000733) and *CD247* (NM_000734.3).

Supplemental Table 3. Primers used for genomic PCR (exons+flanking introns)^A

Gene	Exon	Sequence (5' to 3')	
		Forward	Reverse
<i>CD3D</i>	1	AGCTCTCACCCAGGCTGATAGT	AAGCTCTGGGATTACTGGTGTGA
	2	TGAGCTTCCGCAGAACAAAGG	CACATCCAGAAGCCCTATCCATT
	3	AGGATGGTTCCTGATCTTAAAGG	CACTCTCATGCTCTGCTCTTCCA
	4-5	GGTGGATCTCACAGTCCCATCT	TATATTTATTGGCTGAGCAAGAAGG

^A OLIGO Primer Analysis Software version 7 from Molecular Biology Insights was run for *CD3D* (NG_009891.1)

Supplemental Table 4. Primers and probes used for quantitative PCR^A

Gene	Primer/Probe	Sequence (5' to 3')
<i>CD3DWT</i>	Forward	AGGACAAAGAATCTACCGTGCAA
	Reverse	CACGGTGGCTGGATCCA
	Probe	ATTATCGAATGTGCCAGAGC
<i>CD3DΔEx2</i>	Forward	CGTTTCTCTCTGGCCTGGTACT
	Reverse	CACGGTGGCTGGATCCA
	Probe	ACCCTTCTCTCGCAAGTGTGCCAGA
<i>CD3E</i>	Forward	CAAGGCCAAGCCTGTGAC
	Reverse	TCATAGTCTGGGTTGGGAACA
	Probe	49 (Universal ProbeLibrary for Human, Roche)

^A Primer Express 3.0 from Applied Biosystems was used for *CD3DWT* and *CD3DΔEx2*, and ProbeFinder version 2.40 for Human (Universal ProbeLibrary Assay Design Center) from Roche Applied Science was used for *CD3E*. Sequences as in Supplemental Table 2.

SUPPLEMENTAL METHODS

The S2 *Drosophila* cell reconstitution system

Schneider S2 cells were grown in Schneider's *Drosophila* medium and transfected using CellFectin (Invitrogen Life Technologies) as described (9). Expression vectors for CD3 ϵ , CD3 γ and TCR ζ were generated as described (10) and for TCR α , TCR β , CD3 δ , Δ Ex2 and Δ Ex3 is explained below. After 24 h, protein expression was induced by addition of 1mM CuSO₄ for another 20 h. Subsequently, cells were either stained for flow cytometry or lysed as described (9, 10). For IP 3 μ g of antibody and 5 μ l of protein G-coupled Sepharose (GE Healthcare) was incubated with 300 μ l of cell lysate overnight at 4°C. Beads were washed 3 times in lysis buffer before standard SDS-PAGE and Western blotting.

Generation of *Drosophila* expression vectors

The cDNAs of the proteins of interest were inserted into the *Drosophila* expression vector pRmHa-3 containing an inducible metallothionein promoter (11). pRmHa-3 is abbreviated as pD. The coding sequences of human WT CD3 δ , Δ Ex2 and Δ Ex3 were cloned into the pD vector using EcoRI and XhoI restriction sites from the pIREShrGFPCD3DWT, pIREShrGFPCD3D Δ Exon2 and pIREShrGFPCD3D Δ Exon3 plasmids. Δ Ex3 CD3 δ lacks the transmembrane region and is associated with severe $\alpha\beta$ and $\gamma\delta$ T lymphopenia and SCID (4). pDECPhTCR α HA1.7 and pDECPhTCR β HA1.7, containing sequences that encode for an N-terminally ECFP-tagged HA-specific human TCR α or TCR β chain, were derived from the plasmids pJ6omegaTCR α HA1.7 or pJ6omegaTCR β HA1.7, respectively.

Reconstruction of the TCR complex in *Drosophila* S2 cells

To study TCR assembly, we used the S2 *Drosophila* cell reconstitution system that allows co-transfection and expression of more than 5 different vectors (12). We had used this system previously to reconstruct assembly and surface transport of the BCR complex (13). Here, we firstly show that TCR $\alpha\beta$ dimers do not come to the S2 cell surface if expressed alone, whereas CD3 $\epsilon\delta$ and CD3 $\epsilon\gamma$ do (Supplemental Figure 4A). Co-expression of a CD3 dimer together with TCR $\alpha\beta$ leads to surface expression of TCR $\alpha\beta$, showing that some aspects of TCR assembly and transport to the surface can

be studied using this system (Supplemental Figure 4B). Next, S2 cells were co-transfected with plasmids containing cDNAs of WT CD3 ϵ and WT CD3 δ or Δ Ex2 or Δ Ex3. CD3 proteins were IP from the lysates with a mAb specific for folded CD3 ϵ (OKT3) and a CD3 δ -specific antiserum (M20 δ), separated by non-reducing SDS-PAGE and detected by CD3 δ - or CD3 ϵ -specific antisera by Western blotting (Supplemental Figure 4C). Δ Ex2, but not Δ Ex3, gave rise to a stable protein (bottom left panel) which was able to pair with CD3 ϵ (bottom right panel). The smallest Δ Ex2 form might be a disulphide-linked dimer of nearly the same size as a WT CD3 δ monomer. CD3 ϵ of the Δ Ex2-CD3 ϵ dimers was not folded correctly, since it was not recognized by OKT3 (upper panels), and was aberrantly disulphide bonded to Δ Ex2 (lower left panel). Only WT CD3 δ produced CD3 $\delta\epsilon$ dimers that were recognized by IP using the mAb OKT3 (upper panels) and by flow cytometry using UCHT1 (Supplemental Figure 4D). Furthermore, Δ Ex2 could not diminish expression of a TCR complex (Supplemental Figure 4E), although it was expressed at higher levels than WT CD3 δ (Supplemental Figure 4C bottom left). Therefore, the head-less CD3 δ did not efficiently compete with WT CD3 δ in the formation of a TCR complex. From these results we concluded that Δ Ex2 was unlikely to impinge on $\alpha\beta$ TCR assembly or surface expression in the patients' T cells.

***TCRB* clonality**

Clonality at the *TCRB* locus was studied using a commercial kit (Master Diagnostica, Granada, Spain, EC-certified for clinical use), which amplifies genomic TCR V β J β rearrangements using two primers specific for conserved V and J flanking regions. Polyclonal (normal donor) and monoclonal (Jurkat or MOLT3) control DNAs were included for reference. Amplimers were separated and analyzed in an ABI Prism Genetic Analyzer 3110 using GeneMapper V 4.0 from ABI.

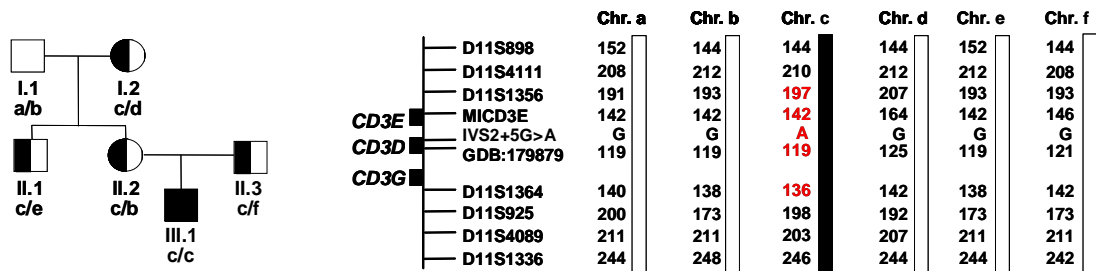
SUPPLEMENTAL FIGURES

Supplemental Figure 1. *CD3D* intron 2 5' splice donor site phylogeny. Multiple alignment of DNA sequences of the gene region surrounding the IVS2+5G>A mutation (arrow) in several mammals (*hominids) reveals that the location of the mutation is conserved. The equivalent location after the exon encoding the extracellular Ig domain is also conserved as a guanine in *CD3G* (not shown).

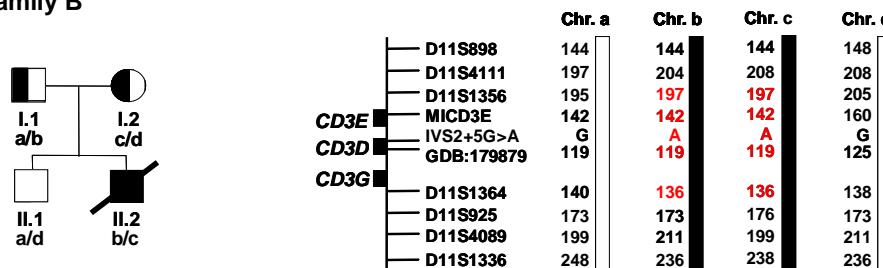
		Splice site ↓
		┌───────────┐
Primates	<i>Homo sapiens*</i>	C G A A g t a c g t g c t
	<i>Pan troglodytes*</i>	- - - - - - - - - - - - - -
	<i>Macaca mulatta</i>	- - - - - - - - t - - - - -
	<i>Macaca fascicularis</i>	- - - - - - - - t - - - - -
Rodents	<i>Mus musculus</i>	- - - - - - - - t - - - - -
	<i>Ratus norvegicus</i>	- - - - - - - - t - - - t -
Horses	<i>Equus caballus</i>	- - - - - - - - t - - - - c
Ruminants	<i>Bos taurus</i>	- - - - - - - - t - - - - -

Supplemental Figure 2. Genetic pedigrees and *CD3* haplotype analysis. Genetic pedigrees of the two families with the *CD3D* mutation. Circles indicate females, squares indicate males (slashed when deceased). Solid symbols denote homozygosity for the mutation, half-solid symbols heterozygosity. *CD3* haplotypes under each symbol are based on the indicated polymorphic markers spanning the *CD3GDE* region on chromosome 11q23. The disease-associated chromosomes are depicted in black with the shared core haplotype markers in red. No genotyping inconsistencies were found. The relative order and the physical distances of markers are as previously reported (1). The allele sizes are normalized with respect to individual 134702, available from Center d'Etude du Polymorphisme Humain (14).

Family A

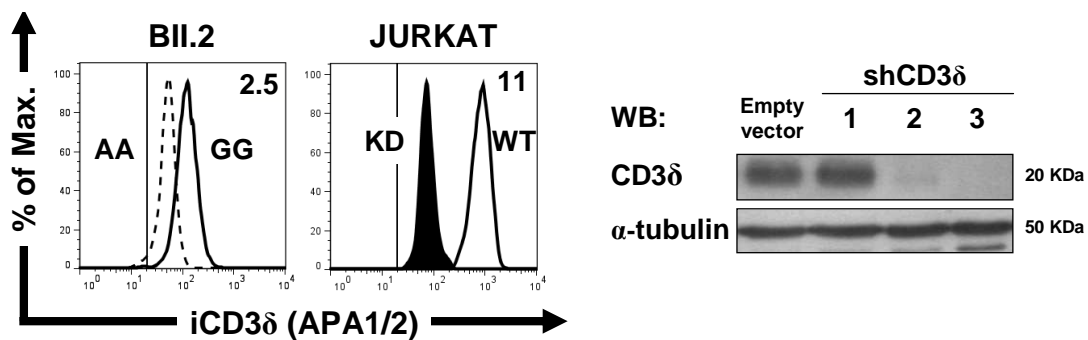


Family B

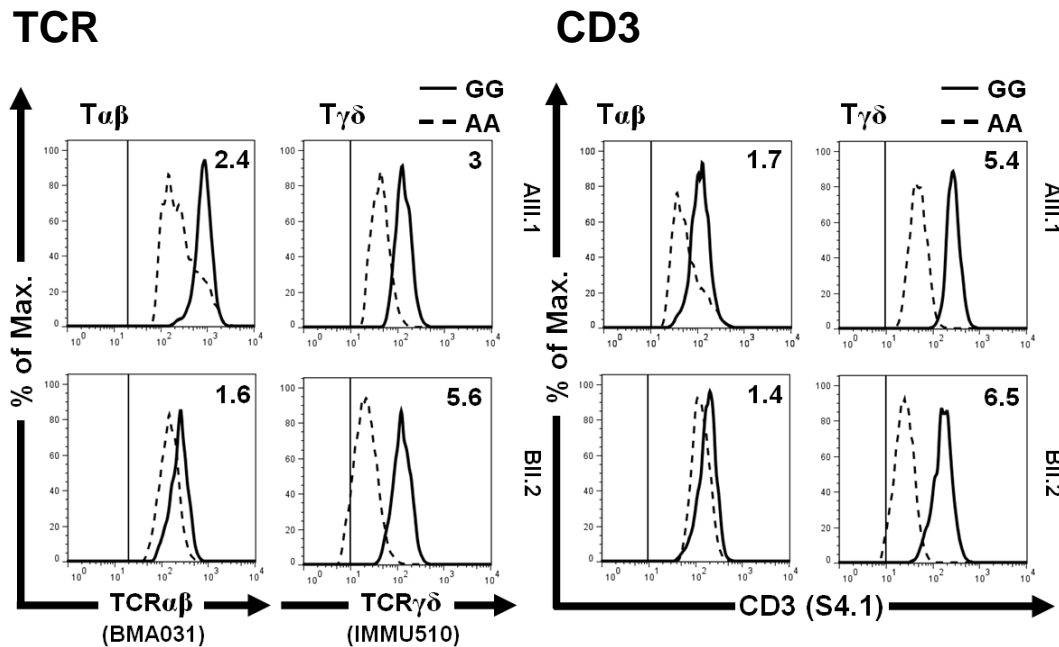


Supplemental Figure 3. TCR complex expression in cultured T cells from patients (dashed lines) or controls (solid lines). (A) Lymphocytes were fixed with 2% paraformaldehyde at 3×10^6 cells/ml for 1 hour at 4°C, permeabilized using 0.2% saponin for 15 minutes at room temperature and stained with APA1/2 (anti-human CD3 δ cytoplasmic tail mAb, 15) followed by anti-mouse IgG-PE (Beckman Coulter). WT Jurkat cells were compared with CD3 δ knock-down (KD) cells using a specific shRNA for CD3 δ RNA which showed a 90% reduction in CD3 δ by Western blotting (right, shCD3 δ 3). The numbers in each histogram indicate the MFI ratios between control and patient or KD. **(B)** Lymphocytes were surface-stained with the indicated TCR- or CD3-specific mAb and analyzed comparatively within the indicated gates. T $\alpha\beta$ cells were defined as BMA031 $^+$, CD3 $^+$ IMMU510 $^-$ or WT31 $^+$, whereas T $\gamma\delta$ cells were defined as IMMU510 $^+$. Histogram numbers as in A.

A Intracellular CD3 δ expression

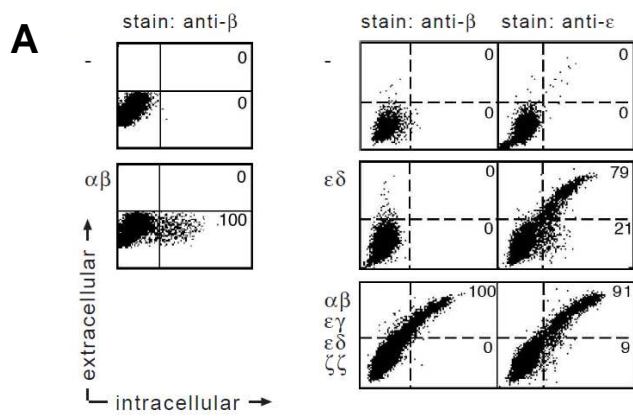


B Surface expression



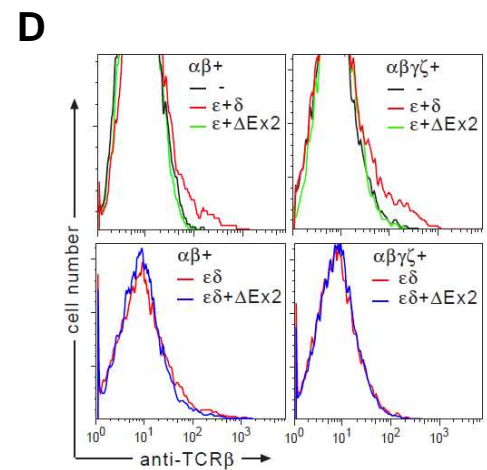
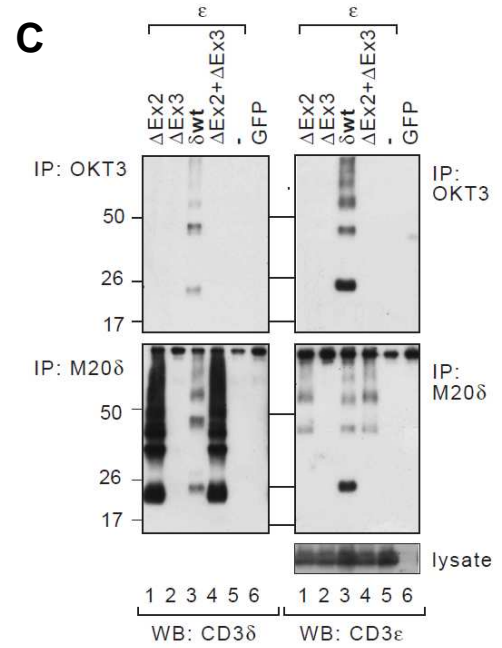
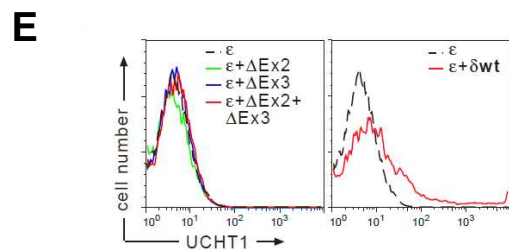
Supplemental Figure 4. Reconstruction of the TCR complex in *Drosophila* S2 cells (A, B, C) to show that Δ Ex2 does not compete with WT CD3 δ to form a TCR complex (D, E). Refer to Supplemental Methods for details.

(A) *Drosophila* S2 cells were transiently transfected with expression plasmids encoding for the indicated proteins or with the empty plasmid (-). After induction with copper sulfate, cells were stained first extracellularly and then after permeabilisation with saponin intracellularly with anti-TCR β (Jovi1, left panels) or anti-folded CD3 ϵ (UCHT1, right panel) antibodies and measured by flow cytometry. (B) Summary of the expression of TCR $\alpha\beta$ (column “ $\alpha\beta$ ”) or CD3 (column “ ϵ ”) on the *Drosophila* S2 cell surface after co-expression of the TCR or CD3 subunits indicated in the left column. Experiments were done as in A) using mouse or human expression plasmids as indicated. - : no expression on the cell surface; + : low and ++ : high expression on the cell surface. As a control, all human TCR and CD3 subunits were expressed as seen by Western blotting (data not shown). Co-expression of a CD3 dimer together with TCR $\alpha\beta$ leads to surface expression of TCR $\alpha\beta$, which was not enhanced upon transfection of all six TCR and CD3 subunits. (C) S2 *Drosophila* cells were transiently transfected with expression plasmids encoding for the indicated proteins (lanes 1-4 and 6) or with the empty plasmid (lane 5). After induction with copper sulfate, the lysates (lowest panel) or anti-folded CD3 ϵ or anti-CD3 δ IP (OKT3, upper panels, or M20 δ , lower panels, respectively) were separated by non-reducing SDS-PAGE. Western blotting was performed with anti-CD3 δ (M20 δ , left panels) or anti-CD3 ϵ (M20 ϵ , right panels) antibodies and the ECL system. (D) S2 cells were transiently transfected with expression plasmids encoding for the indicated proteins. After induction with copper sulfate, cells were stained with the anti-TCR β antibody Jovi3 and measured by flow cytometry. (E) S2 cells were transiently transfected with expression plasmids encoding for the indicated proteins (coloured lines) or with the empty plasmid (black lines). After induction with copper sulfate, cells were stained with the anti-folded CD3 ϵ antibody UCHT1 and measured by flow cytometry.

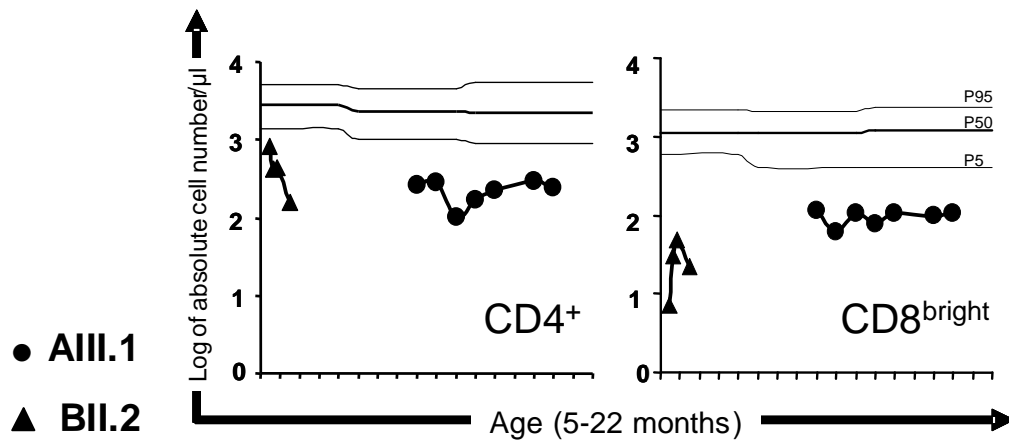


B

co-expression	mouse		human	
	$\alpha\beta$	ϵ	$\alpha\beta$	ϵ
$\alpha\beta$	-		-	
$\epsilon\gamma$		++		++
$\epsilon\delta$		++		++
$\alpha\beta \epsilon$	-		-	
$\alpha\beta \gamma$	-		-	
$\alpha\beta \delta$	-		-	
$\alpha\beta \epsilon\gamma$	++	++	+	+
$\alpha\beta \epsilon\delta$	++	++	++	++
$\alpha\beta \zeta\zeta$	-		-	
$\alpha\beta \epsilon\gamma \epsilon\delta$	++	++	++	++
$\alpha\beta \epsilon\gamma \epsilon\delta \zeta\zeta$	++	++	++	++

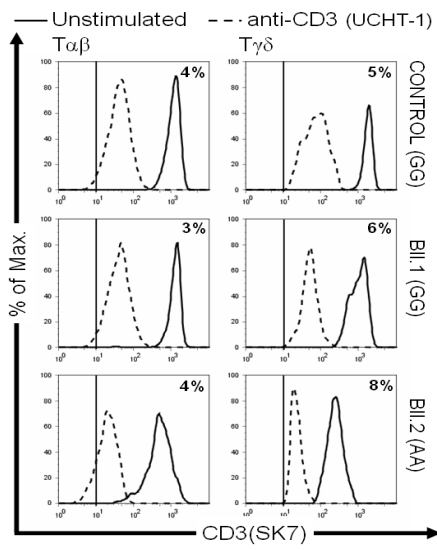


Supplemental Figure 5. T $\alpha\beta$ lymphocyte subset numbers. Absolute CD4⁺ and CD8^{bright} cell numbers in patients (AIII.1 dots, BII.2 triangles) plotted as a function of age in comparison with the normal age-matched distribution (P5, P50 and P95, 16).

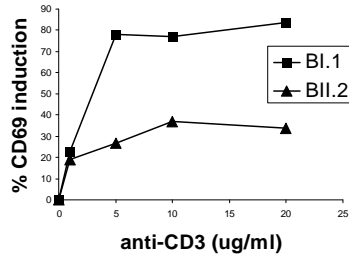


Supplemental Figure 6. TCR complex function. (A) TCR down-regulation after 24 hours in response to anti-CD3 stimulation in primary T $\alpha\beta$ (CD4⁺) or T $\gamma\delta$ (11F2⁺) lymphocytes with the indicated *CD3D* IVS2+5 genotypes. The numbers in each histogram indicate CD3 MFI percentages of stimulated (dashed lines) relative to unstimulated cells (solid lines). (B) CD69 induction (% expression) in T cell lines from the indicated donors after stimulation with different amounts of UCHT-1 for 24 hours. (C) CD25 induction after 36 hours in stimulated (dashed lines) compared to unstimulated (solid lines) primary CD4⁺ T cells (mostly T $\alpha\beta$ cells). The numbers in each histogram indicate MFI increments normalized to control cell increments. (D) Lymphocyte proliferation was evaluated by flow cytometry using CFSE dye dilution (17). CFSE-labeled peripheral blood lymphocytes were cultured for 5 days in the presence (+) or absence (–) of phytohemagglutinin (PHA, left) or the anti-CD3 antibody UCHT-1 (right). Cells were analyzed for CFSE dilution by flow cytometry within the indicated subsets. In this experiment T $\alpha\beta$ and T $\gamma\delta$ lymphocytes were defined as CD4⁺ (>98% T $\alpha\beta$ cells), and double negative CD3⁺ (78±6% T $\gamma\delta$ cells) because the TCR was down-regulated after activation.

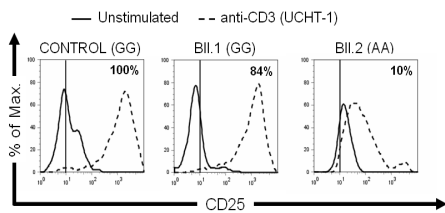
A TCR down-regulation



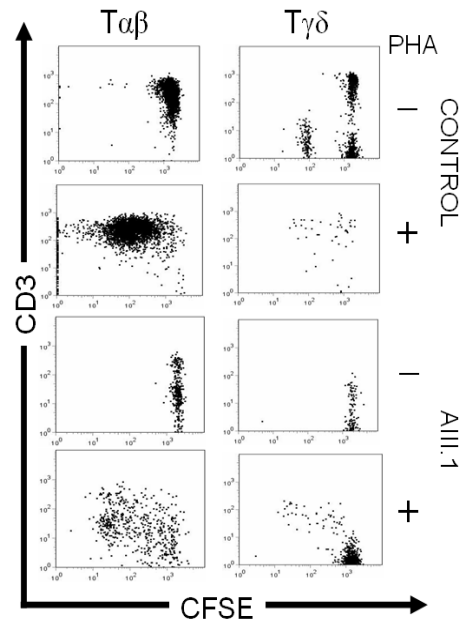
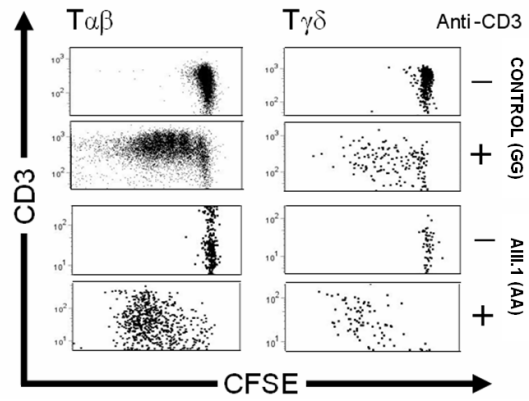
B CD69 induction



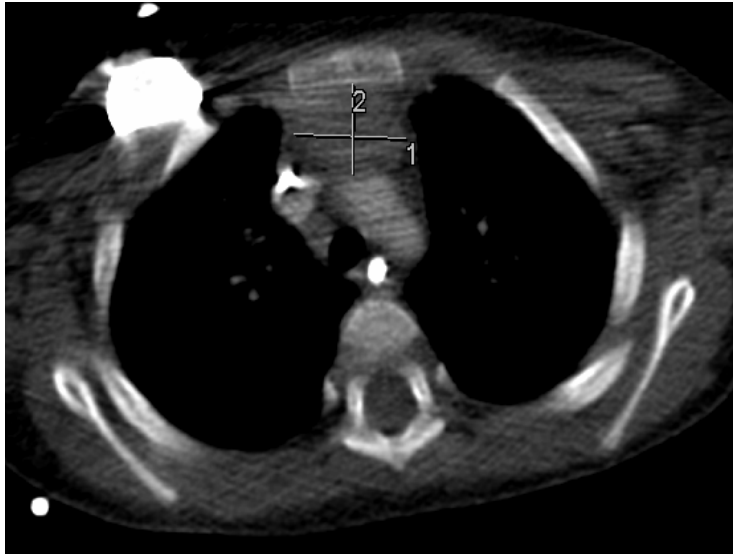
C CD25 induction



D Lymphocyte proliferation

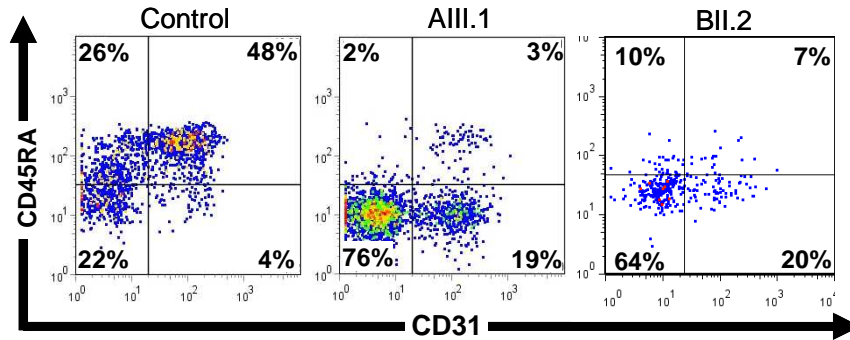


Supplemental Figure 7. Thymus of patient AIII.1 at diagnosis (chest CT scan). Patient AIII.1 showed a thymus of 2.39 x 1.8 cm (1 and 2 in image, respectively), within the normal age-matched dimensions \pm SD of 3.13 ± 0.85 x 2.52 ± 0.82 (18). In patient BII.2 the thymus was initially not detected by CT scan, but his necropsy revealed the presence of a thymus remnant of 2 x 1 cm.

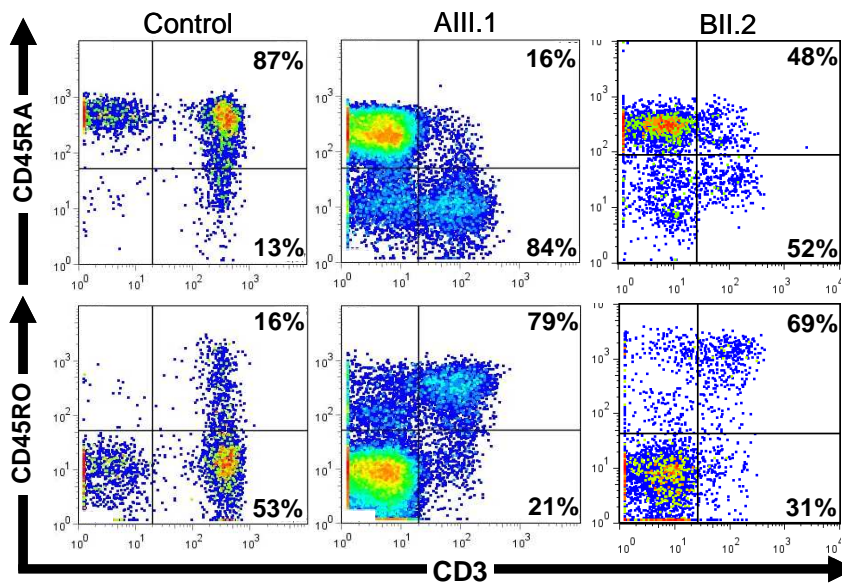


Supplemental Figure 8. T lymphocyte phenotype in the patients to a normal age-matched control. (A) Recent thymic emigrants defined as $CD4^+CD45RA^+CD31^+$ T cells (19). (B) $CD45RA^+$ (naïve) and $CD45RO^+$ (memory) T lymphocytes. (C) CD25 expression in patients with *CD3D* IVS2+5 AA genotype (dashed lines) in comparison with controls (GG, solid lines) in $T\alpha\beta$ cells defined as $CD4^+$ and in $T\gamma\delta$ cells defined as $11F2^+$.

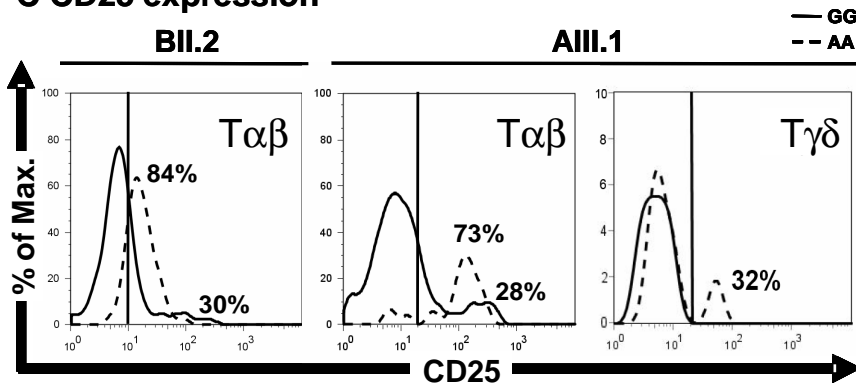
A Recent $CD4^+$ thymic emigrants



B $CD45RA^+/CD45RO^+$ T lymphocytes

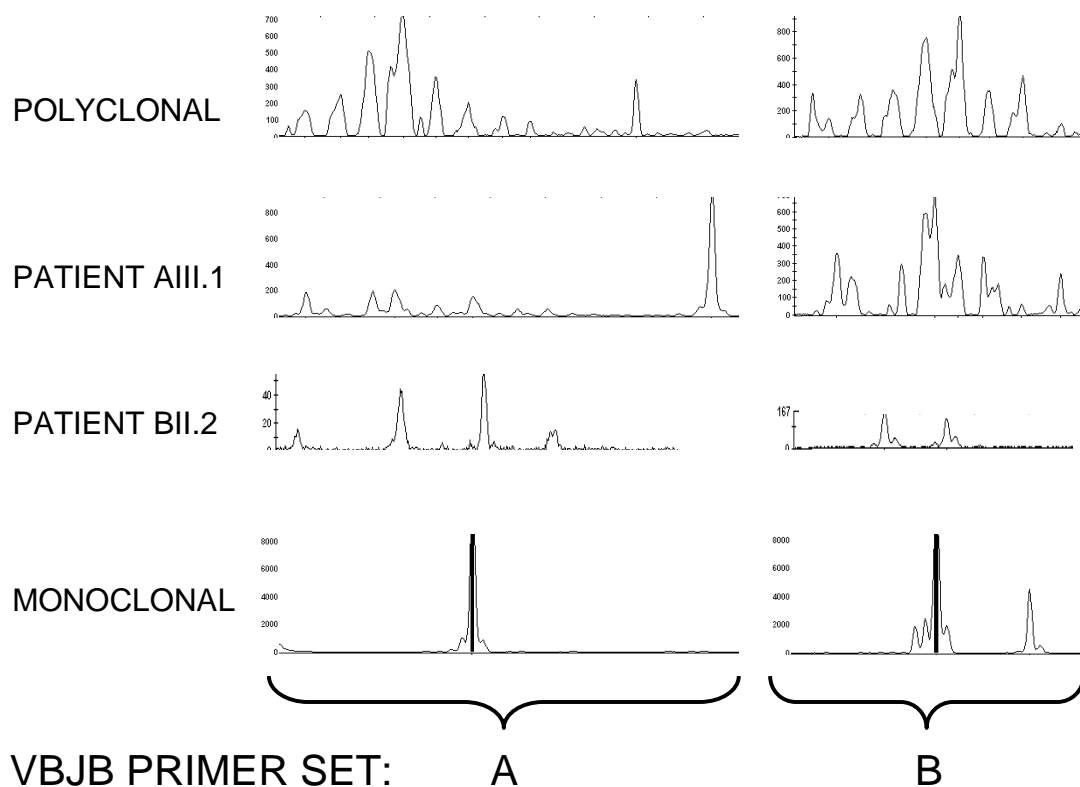


C CD25 expression



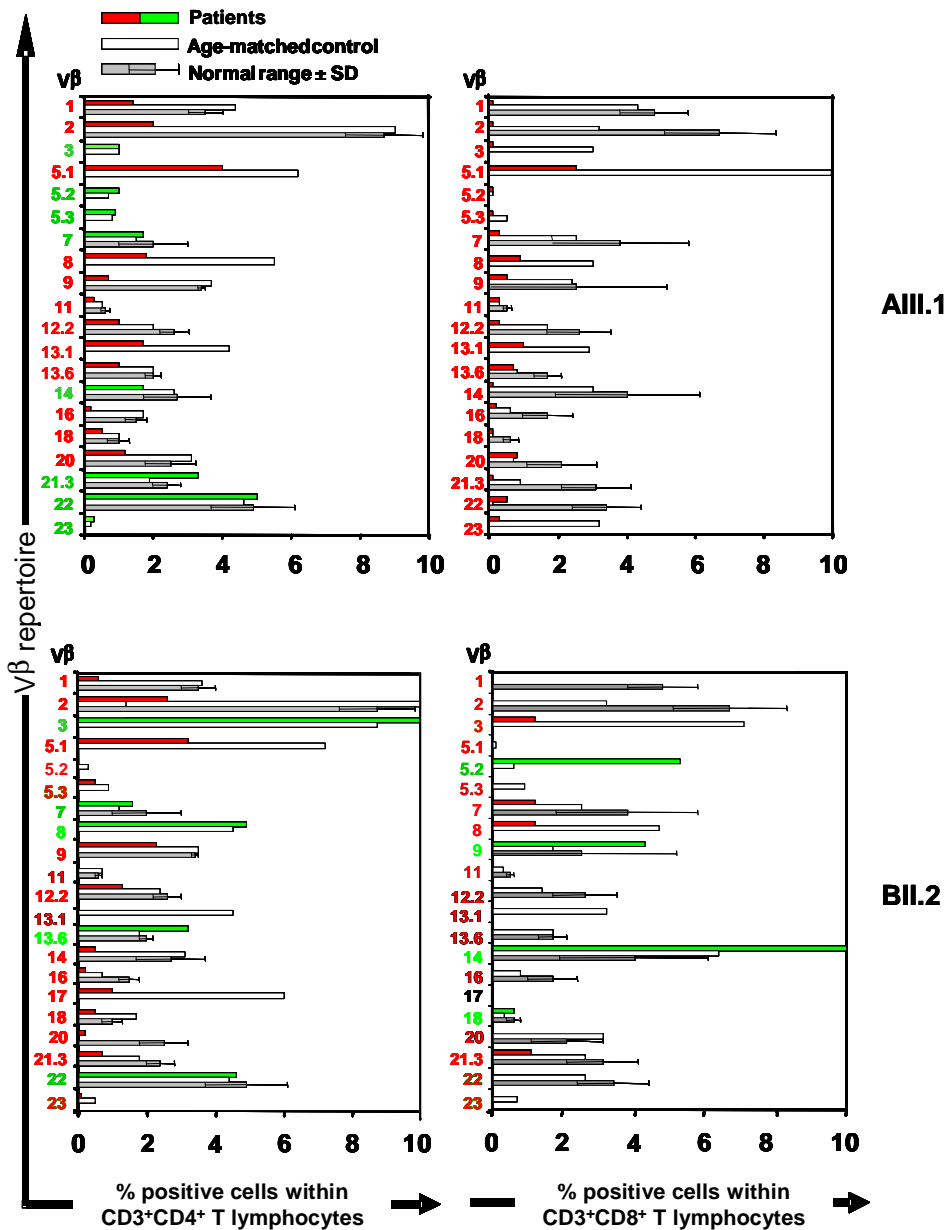
Supplemental Figure 9A. *TCRB* clonality. Genomic *TCR V β J β* rearrangements were amplified in the patients using two different primer sets (VBJB-A and -B) and compared with a normal (polyclonal) donor and two tumoral T cell lines (monoclonal) in the 240-280 bp range. The two primer sets are specific for conserved V and J flanking regions, and therefore amplify genomic *TCR V β J β* rearrangements as fragments of the indicated size range (see Supplemental Methods in page 4). Normal T lymphocytes are polyclonal and thus show a Gaussian fragment distribution (POLYCLONAL in Figure). T lymphoid tumors such as Jurkat or MOLT3 are monoclonal and thus yield a single major peak (MONOCLONAL in Figure). Patients with poor *TCR β* diversity show few peaks without Gaussian distribution.

A *TCRB* clonality



Supplemental Figure 9B. TCRV β repertoire within CD4⁺ and CD8⁺ T populations by flow cytometry using a collection of anti-TCR V β antibodies from Beckman Coulter Immunotech. Data are shown within range (green) or out of range (red) (black, not done) in comparison with a normal age-matched control (empty bars) and the normal range (grey bars \pm SD, 20).

B TCR V β repertoire within T lymphocyte subsets



SUPPLEMENTAL REFERENCES

1. Recio MJ, et al. Differential biological role of CD3 chains revealed by human immunodeficiencies. *J Immunol.* 2007;178(4):2556-64.
2. Dadi HK, Simon AJ, Roifman CM. Effect of CD3delta deficiency on maturation of alpha/beta and gamma/delta T-cell lineages in severe combined immunodeficiency. *N Engl J Med.* 2003;349(19):1821-28.
3. de Saint Basile G, et al. Severe combined immunodeficiency caused by deficiency in either the delta or the epsilon subunit of CD3. *J Clin Invest.* 2004; 114(10):1512-17.
4. Takada H, Nomura A, Roifman CM, Hara T. Severe combined immunodeficiency caused by a splicing abnormality of the CD3delta gene. *Eur J Pediatr.* 2005;164(5):311-14.
5. Soudais C, Villartay J P, Deist F L, Fischer A, Lisowska-Grospierre B. Independent mutations of the human CD3-epsilon gene resulting in a T cell receptor/CD3 complex immunodeficiency. *Nat Genet* 3:77-81, 1993
6. Roberts JL, et al. T^B⁺NK⁺ severe combined immunodeficiency caused by complete deficiency of the CD3zeta subunit of the T-cell antigen receptor complex. *Blood.* 2007;109(8):3198-206.
7. Rieux-Laucat F, Hivroz C, Lim A, et al. Inherited and somatic CD3zeta mutations in a patient with T-cell deficiency. *N Engl J Med* 2006; 354: 1913-21.
8. Morgan NV, et al. Mutation in the TCR α subunit constant gene (TRAC) leads to a human immunodeficiency disorder characterized by a lack of TCR $\alpha\beta$ ⁺ T cells. *J Clin Invest.* 2011;121(2):695-702.
9. Swamy M, Kulathu Y, Ernst S, Reth M, Schamel WW. Two dimensional Blue Native-/SDS-PAGE analysis of SLP family adaptor protein complexes. *Immunol Lett.* 2006;104(1-2):131-7.
10. Dopfer EP, et al. Analysis of novel phospho-ITAM specific antibodies in a S2 reconstitution system for TCR-CD3 signalling. *Immunol Lett.* 2010;130(1-2):43-50.
11. Bunch TA, Grinblat Y, Goldstein LS. Characterization and use of the Drosophila metallothionein promoter in cultured Drosophila melanogaster cells. *Nucleic Acids Res.* 1988;16(3):1043-61.
12. Rolli V, et al. Amplification of B cell antigen receptor signaling by a Syk/ITAM

- positive feedback loop. *Mol Cell*. 2002;10(5):1057-69.
13. Schamel WW, Kuppig S, Becker B, Gimborn K, Hauri HP, Reth, M. A high molecular weight complex of BAP29/BAP31 is involved in the retention of membrane-bound IgD in the endoplasmic reticulum. *Proc Natl Acad Sci*. 2003; 100(17):9861-66.
 14. Dib C, et al. A comprehensive genetic map of the human genome based on 5,264 microsatellites. *Nature*. 1996;380(6570):152-4.
 15. Alarcón A, et al. The CD3 γ and CD3 δ subunits of the T cell antigen receptor can be expressed within distinct functional TCR/CD3 complex. *EMBO J*. 1991;10(4): 903-12.
 16. Comans-Bitter WM, et al. Immunophenotyping of blood lymphocytes in childhood. Reference values for lymphocyte subpopulations. *J Pediatr*. 1997; 130(3):388-93.
 17. Lyons AB. Analysing cell division in vivo and in vitro using flow cytometric measurement of CFSE dye dilution. *J Immunol Methods*. 2000;243(1-2):147-54.
 18. Francis IR, Glazer GM, Bookstein FL, Gross BH. The thymus: Reexamination of age-related changes in size and shape. *AJR Am J Roentgenol*. 1985;145(2): 249-54.
 19. Kohler S, Thiel A. Life after the thymus: CD31 $^{+}$ and CD31 $^{-}$ human naïve CD4 $^{+}$ T-cell subsets. *Blood*. 2009;113(4):769-74.
 20. van den Beemd R, et al. Flow Cytometric Analysis of the V β Repertoire in Healthy Controls. *Cytometry*. 2000;40(4):336-45.